NeuroImage 56 (2011) 235–245

Contents lists available at ScienceDirect

NeuroImage

journal homepage: www.elsevier.com/locate/ynimg

Age-related alterations in the modular organization of structural cortical network by using cortical thickness from MRI

Zhang J. Chen [a], Yong He [b], Pedro Rosa-Neto [c], Gaolang Gong [a], Alan C. Evans [a,*]

[a] McConnell Brain Imaging Centre, Montréal Neurological Institute, McGill University, Montreal, Canada
[b] State Key Laboratory of Cognitive Neuroscience and Learning, Beijing Normal University, Beijing, China
[c] Department of Neurology & Neurosurgery and Psychiatry, McGill University, Montreal, Canada

ARTICLE INFO

Article history:
Received 13 August 2010
Revised 3 January 2011
Accepted 5 January 2011
Available online 14 January 2011

ABSTRACT

Normal aging is accompanied by various cognitive functional declines. Recent studies have revealed disruptions in the coordination of large-scale functional brain networks such as the default mode network in advanced aging. However, organizational alterations of the structural brain network at the system level in aging are still poorly understood. Here, using cortical thickness, we investigated the modular organization of the cortical structural networks in 102 young and 97 normal aging adults. Brain networks for both cohorts displayed a modular organization overlapping with functional domains such as executive and auditory/language processing. However, compared with the modular organization of young adults, the aging group demonstrated a significantly reduced modularity that might be indicative of reduced functional segregation in the aging brain. More importantly, the aging brain network exhibited reduced intra-/inter-module connectivity in modules corresponding to the executive function and the default mode network of young adults, which might be associated with the decline of cognitive functions in aging. Finally, we observed age-associated alterations in the regional characterization in terms of their intra/inter-module connectivity. Our results indicate that aging is associated with an altered modular organization in the structural brain networks and provide new evidence for disrupted integrity in the large-scale brain networks that underlie cognition.

Introduction

Normal aging is accompanied by various cognitive functional declines such as executive skills and memory. Previous neuroimaging studies in aging have suggested those deficits might arise from various focal abnormalities such as decreased grey matter density (Sowell et al., 2003) and cortical thickness (Salat et al., 2004; Fjell et al., 2009), and alterations in functional/structural brain systems (Grady et al., 2003; Salat et al., 2005; Andrews-Hanna et al., 2007), possibly due to subtle anatomical disconnections between functionally-coordinated brain regions (O'Sullivan et al., 2001). Furthermore, using advanced graph theoretical analysis (Watts and Strogatz, 1998), aging brain structural and functional network have also been shown to display altered network characteristics such as decreased efficiency that are essential in sustaining both segregated and integrated information processing in the normal brain system (Achard and Bullmore, 2007; Gong et al., 2009; Zhu et al., 2010). However, most recent studies in aging brain networks have focused on the global scale (e.g. efficiency) or regional level (e.g. nodal centrality). It remains unclear how the intrinsic modular organization of brain network is affected in aging.

Modularity is a fundamental and ubiquitous network property that underlies the functionality of most complex systems in nature, ranging from social to biological networks such as the air transportation (Guimera et al., 2005) and metabolic networks (Guimera and Nunes Amaral, 2005). Network modularity is defined by the existence of distinct groups of nodes with more dense connections with each other than with the others in the network. Detecting modularity in a network helps to identify relevant substructures that subserve specific functions, thus providing a link between structure and function (Fortunato and Barthelemy, 2007). One hypothesis is that modularity might arise from the evolutionary constraints wherein a complex system is driven by the need for rapid adaptation to a changing environment by altering the key functions (modules) without affecting other functions (Variano et al., 2004; Kashtan and Alon, 2005).

In neuroscience, modular network analysis has provided rich quantitative insights into the organization of complex brain networks. Studies in mammalian anatomical brain networks have revealed clusters that overlap with many known brain functions

* Corresponding author. McConnell Brain Imaging Centre, Montreal Neurological Institute, Montreal, QC, Canada H3A 2B4. Fax: +1 514 398 8948.
E-mail address: alan.evans@mcgill.ca (A.C. Evans).

1053-8119/$ – see front matter © 2011 Elsevier Inc. All rights reserved.
doi:10.1016/j.neuroimage.2011.01.010

(Hilgetag et al., 2000b; Zhou et al., 2006). Previous neuoimaging studies have also demonstrated anatomically- and functionally-related modules in both the human brain structural network using diffusion spectra imaging (Hagmann et al., 2008) and the functional network using functional MRI (Salvador et al., 2005; Ferrarini et al., 2009; He et al., 2009; Valencia et al., 2009). Several recent functional brain network studies have also demonstrated disruption of several large-scale brain systems such as the executive control, dorsal attention system and default mode network in aging (Andrews-Hanna et al., 2007; Damoiseaux et al., 2008; Madden et al., 2010). Moreover, a network-based functional/structural neuroimaging study has revealed neurodegenerative diseases such as Alzheimer's disease (AD), also target specific large-scale distributed brain systems (Seeley et al., 2009). Another recent study has demonstrated a reduced number of inter-module connections to the frontal regions in the functional brain network in normal aging as compared to those of the young adults (Meunier et al., 2009). In our previous study, using regional cortical thickness, we demonstrated the modular organization of the human brain structural network (Chen et al., 2008). More importantly, the cortical network modules identified are composed of brain regions known to subserve distinct functions such as language, motor control and vision (Chen et al., 2008). However, it remains unclear how this modular organization might be affected in aging. Therefore, our main hypotheses are that, compared with the modular structures of the young adults, the normal aging brain network would demonstrate: a) a reduced modularity, b) a reduction in the connectivity of the modules corresponding to both the executive and default mode network functions, and c) a reduction of the connectivity between the anterior and posterior modules. To test these hypotheses, we analyzed the modular organization of cortical structural networks in two cohorts, 102 young adults and 97 older adults. To our knowledge, this is the first study to characterize the age-related changes in the modular organization of the brain structural network by using cortical thickness correlation analysis.

Materials and methods

Subjects

One hundred and ninety-nine right-handed subjects were selected from the Open Access Series of Imaging Studies (OASIS) database (http://www.oasis-brains.org) including 102 young adults (41 females and 61 males) age ranged from 20 to 27 (mean = 22.3; SD = 1.92) and 97 healthy elders (71 females and 26 males) age ranged from 60 to 94 (mean = 75.93; SD = 9.03). Young and middle-aged adults were questioned before image acquisition about their medical histories and use of psychoactive drugs and older adults (aged 60 and older), underwent the ADRC's (Washington University Alzheimer Disease Research Center) full clinical assessment (Marcus et al., 2007). Dementia status was established and staged using CDR scale (Morris, 1993; Morris et al., 2001) with CDRs of 0, 0.5, 1, 2, and 3 represent no dementia, very mid, mid, moderate, and severe dementia, respectively. Only the normal aging subjects (CDR = 0) were applied in this study. For a more detailed clinical and demographic data of all subjects, see Marcus et al., 2007.

Image acquisition

Three to four T1-weighted structural MR images were collected for each subject. MRI scans were performed on a Siemens 1.5 T Vision scanner [repetition time = 9.7 ms; echo time = 4.0 ms; inversion time = 20 ms; delay time = 200 ms; flip angle = 10°; orientation, sagittal; resolution = 256 × 256 matrix (1 × 1 mm); slices = 128; thickness = 1.25 mm] within a single session. However, the T1 image we obtained from the OASIS database for each subject was an average image (1 × 1 × 1 mm) that was a motion-corrected coregistered average of all available data (Marcus et al., 2007). For a more detailed postprocessing of the image, see Marcus et al., 2007.

Cortical thickness measurement

Cortical thickness measurement procedures have been previously reported in several studies (MacDonald et al., 2000; Kim et al., 2005). In brief, native structural MR image of each subject was corrected for nonuniformity (Sled et al., 1998), linearly registered into stereotaxic space (Collins et al., 1994) and segmented into gray matter, white matter, cerebrospinal fluid (CSF) and background using a neural net classifier (Zijdenbos et al., 2002). The inner and outer gray matter surfaces composed of 40,962 vertices for each hemisphere were then automatically extracted using the constrained Laplacian based automated segmentation with proximities (CLASP) algorithm (MacDonald et al., 2000; Kim et al., 2005). Cortical thickness was defined as the distance between the same vertex on the inner and outer surfaces (Lerch and Evans, 2005). The resulting mean cortical thickness maps for both the young adults and normal aging groups are shown in Fig. 1A.

Anatomical parcellation

Each structural MRI dataset was nonlinearly registered (Collins et al., 1995; Robbins et al., 2004) to a presegmented and validated volumetric template and segmented using the automated anatomical labeling (AAL) atlas (Tzourio-Mazoyer et al., 2002) as shown in Fig. 1B. This parcellation divided the cortical surface into 78 regions (left hemisphere: 39, right hemisphere: 39). See Table 1 for the name of the regions and their corresponding abbreviations.

Structural brain network construction

In brain connectivity studies, structural and functional brain networks are commonly defined as a set of brain regions linked by either structural (fibre track, morphological) or functional (correlated activation during task or time series correlations in resting state) connections, respectively. Accordingly, the structural brain network defined in this study is derived from a 78 × 78 correlation matrix computed from 78 mean regional cortical thickness. The procedure of brain network construction was similar to that used in our previous study (He et al., 2007). Briefly, the average regional thickness of the 78 cortical regions was generated by averaging all vertices with the same anatomical label (highest occurrence). Before measuring the correlations between regions, a linear regression was performed at every cortical region to remove the effects of age, gender, age-gender interaction and mean cortical thickness; the resulting residuals were used to substitute for the raw cortical thickness values. Finally, the full-weighted brain structural networks (78 × 78) for both the young and aging groups were obtained by calculating the absolute Pearson correlation coefficients across individuals between the cortical thicknesses of every pair of regions. The structural cortical networks for both the young and aging groups are shown in Fig. 1C.

Weighted brain network analysis

The resulted correlation matrix obtained in previous step was directly applied as a continuously-weighted network G with N (78) nodes and K (3003, 78 × 77/2) possible weighted edges, where nodes represent cortical regions and edges represent undirected connections between regions. For group comparison, edge weights in both the young and aging brain networks were normalized by their total network weight (total cost is normalized to unity for both networks) which is similar to the cost control in a binarized network analysis that imposes the same number of edges.

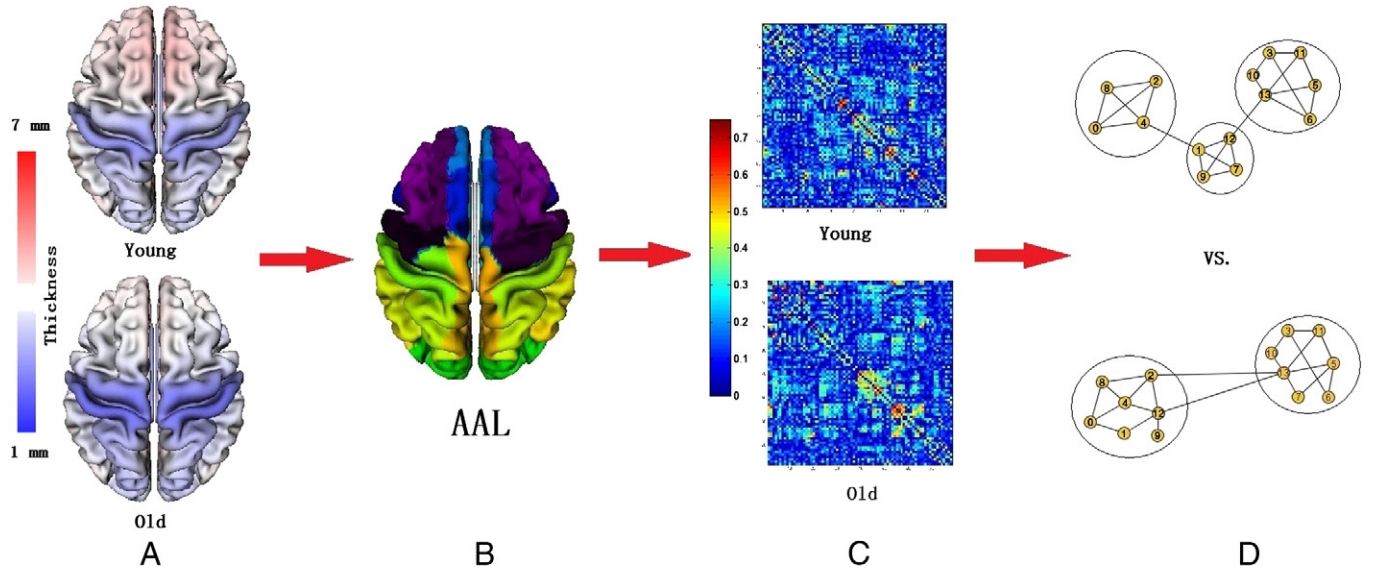

Fig. 1. Flowchart for the construction/analysis of the structural cortical networks in young adults and normal aging groups. (A) Thickness of the 78 cortical regions for both the young adults and aging groups was generated by averaging all vertices with the same anatomical label after resampling individual cortical surface to the predefined AAL template surface. (B) (C). The inter-regional cortical thickness correlation matrix (78×78) across subjects within each group. The color bar represents the weight of the network (see Materials and methods). (D) The modular organization of weighted cortical structural networks for both the young adults and aging groups were analyzed.

Identification of network modules

The modules of the structural brain network defined in the study (78×78) is referring to the groups of tightly clustered cortical regions in thickness. The modularity $Q(p)$ for a given partition p of the full-weighted brain structural network is defined as:

$$Q(p) = \sum_{s=1}^{N_M} \left[\frac{w_s}{W} - \left(\frac{W_s}{2W} \right)^2 \right] \quad (1)$$

where N_M is the number of modules, W is the total weight of the network, w_s is the sum of the connectional weights between all nodes in module s, and W_s is the sum of the nodal weights in module s. The modularity index quantifies the difference between the weight of intra-module links of the actual network and that of random networks in which connections are weighted at random (Newman, 2004). The aim of this module identification process is to find a specific partition p which yields the largest network modularity, $Q(p)$. We use a modified greedy optimization algorithm (Clauset et al., 2004; Danon et al., 2006) to find the modules of the network. The advantage of this modularity optimization method is that it takes into account of the heterogeneity of module size observed in real networks (Danon et al., 2006). This optimization procedure was described in more detail in Chen et al., 2008.

Intra- and inter-module connectivity

We refer to the intra-module connectivity of module, s, within its network as MC_s; where MC_s is the sum of all connectional weights within module s. A higher value of MC indicates a greater significance of the corresponding module within the whole network. We also refer to the inter-module connectivity between modules s and t as IMC_{st}; where IMC_{st} is the sum of connectional weights between the modules s and t. Higher value of IMC suggests a stronger connection between the two corresponding modules.

Table 1
Parcellation of 78 AAL cortical surface regions and their abbreviations (odd number: left hemisphere, even number: right hemisphere).

#	Regions	Abbr.	#	Regions	Abbr.
1, 2	Precentral gyrus	PreCG	41, 42	Cuneus	CUN
3, 4	Superior frontal gyrus (dorsal)	SFGdor	43, 44	Lingual gyrus	LING
5, 6	Orbitofrontal cortex (superior)	ORBsup	45, 46	Superior occipital gyrus	SOG
7. 8	Middle frontal gyrus	MFG	47, 48	Middle occipital gyrus	MOG
9, 10	Orbitofrontal cortex (middle)	ORBmid	49, 50	Inferior occipital gyrus	IOG
11, 12	Inferior frontal gyrus (opercular)	IFGoperc	51, 52	Fusiform gyrus	FFG
13, 14	Inferior frontal gyrus (triangular)	IFGtriang	53, 54	Postcentral gyrus	PoCG
15, 16	Orbitofrontal cortex (inferior)	ORBinf	55, 56	Superior parietal gyrus	SPG
17, 18	Rolandic operculum	ROL	57, 58	Inferior parietal lobule	IPL
19, 20	Supplementary motor area	SMA	59, 60	Supramarginal gyrus	SMG
21, 22	Olfactory	OLF	61, 62	Angular gyrus	ANG
23, 24	Superior frontal gyrus (medial)	SFGmed	63, 64	Precuneus	PCUN
25, 26	Orbitofrontal cortex (medial)	ORBmed	65, 66	Paracentral lobule	PCL
27, 28	Rectus gyrus	REC	67, 68	Heschl gyrus	HES
29, 30	Insula	INS	69, 70	Superior temporal gyrus	STG
31, 32	Anterior cingulate gyrus	ACG	71, 72	Temporal pole (superior)	TPOsup
33, 34	Middle cingulate gyrus	MCG	73, 74	Middle temporal gyrus	MTG
35, 36	Posterior cingulate gyrus	PCG	75, 76	Temporal pole (middle)	TPOmid
37, 38	Parahippocampal gyrus	PHG	77, 78	Inferior temporal gyrus	ITG
39, 40	Calcarine cortex	CAL			

Regional intra- and inter-module connectivity

We determined the intra-module degree and participation coefficient for each cortical region as indices of their intra- and inter-module connection density, repectively (Guimera and Amaral, 2005; Guimera and Nunes Amaral, 2005; Sales-Pardo et al., 2007). The intra-module degree, z_i, measures the regional intra-module connectivity of node *i*, and is defined as:

$$z_i = \frac{w_i - \overline{W}_s}{\sigma_s} \quad (2)$$

where w_i is the intra-module weight of a node *i*, within module, *s*. $\overline{W}_s$ is the average intra-modular weight of all nodes in module *s*. σ_s is the standard deviation of intra-modular weight of all nodes in module *s*. A high value of within-module degree *Zi* indicates strong intra-modular connectivity for node *i*.

The participation coefficient, P_i, measures the regional inter-module connectivity of node *i*, and is defined as:

$$P_i = 1 - \sum_{s=1}^{N_M} \left(\frac{w_{is}}{w_i}\right)^2 \quad (3)$$

where N_M is the number of modules and w_{is} is inter-modular connectional weight between the node *i* and module *s*. w_i is the total weight of node *i* in the network. The participation coefficient of node *i* will be close to 0 if all weights are largely intra-modular. In our present study, since our network is full-connected, the *P* will always have a relatively higher value compared to other studies (Guimera and Nunes Amaral, 2005; Meunier et al., 2009).

Statistical analysis

In order to evaluate the significance of the network modularity, we compared the network modularity obtained from real brain data with those of 1000 randomly-generated networks created by randomly-reassigning the edge weights within the same set of nodes. We defined the *z*-score as $(Q_{real} - Q_{rand})/Q_{std}$, where Q_{real} is the maximum modularity of the cortical network, and Q_{rand} and Q_{std} are the mean and standard deviation of the maximum modularity over all randomized networks respectively.

To determine the statistical significance of the between-group differences in network parameters, we applied a non-parametric permutation test method (Bullmore et al., 1999; He et al., 2008). First, *all* network parameters (e.g. intra/inter-module connectivity) were computed separately for the young adults and normal aging cohort. We then randomly reassigned the regional cortical thickness measures of each subject to either cohort and recomputed the correlation matrix for each randomized cohort. The network parameters were then re-calculated and their between-group differences were obtained. This randomization procedure was repeated 1000 times and the 95 percentile values of each distribution were used as the critical values for a one-tailed test of the null hypothesis as the *p* values were calculated as the proportion of entries in the permutation distribution that were either greater or less than observed between-group difference.

To test whether interregional correlation of cortical thickness was significantly different between the young and elder groups, correlation coefficients were further converted into *z* values by using Fisher's *r*-to-*z* transform. This transformation generated values that were approximately normally distributed and a *Z* statistic was then used to compare these transformed *z* values to determine the significance of the between-group differences in correlations (Cohen and Cohen, 1983). To adjust for the multiple comparisons, a false discovery rate (FDR) procedure was performed at a *q* value of 0.05 (Genovese et al., 2002).

Results

Modular structures of the young adults brain network

Five functionally oriented modules were uncovered in the young adults brain network as shown in Fig. 2A. 1) Module I (Fig. 2A.I) includes 5 regions from left-hemisphere frontal lobe such as superior frontal gyrus (SFGdor), middle frontal gyrus (MTG), medial frontal gyrus (SFGmed) and anterior cingulum gyrus (ACG) which are mainly corresponding to the executive brain function (Duncan and Owen, 2000). 2) Module II includes 19 regions that are mainly associated with auditory/language function such as inferior frontal gyrus (IFGtriang and IFGoperc), supermarginal gyrus (SMG) and superior temporal gyrus (STG) (Mesulam, 1990). 3) The third module (Fig. 2A. III) is composed of 15 regions which are mostly along the ventral visual (occipital–temporal) pathway [e.g. inferior occipital gyrus (IOG), inferior temporal gyrus (ITG), fusiform gyrus (FFG)] that might be related to the visual integration function (object recognition) of the brain (Grill-Spector, 2003; Ison and Quiroga, 2008). 4) The 21-region module IV (Fig. 2A.IV) includes mostly orbital–frontal, cingulum and parietal regions such as bilateral superior orbital–frontal (ORBsup), middle cingulum (MCG), posterior cingulum (PCG) and precunus (PCUN) which are the main components of the default mode network of the brain (Raichle et al., 2001; Greicius et al., 2003). 5) The 18-region module V consists of regions from parietal [e.g. superior parietal gyrus (SPG) and postcentral gyrus (PoCG)], occipital [e.g. superior occipital gyrus (SOG) and middle occipital gyrus (MOG)] and frontal [e.g. precentral gyrus (PrCG)] lobes that are mainly related to the sensorimotor/visual/spatial function (Mesulam, 2000).

Modular structures of the normal aging brain network

In the elder adult brain network, we detected four major modules labeled from I to IV when the maximum modularity was reached as shown in Fig. 2B. 1) Module I consists of 8 regions from frontal areas such as bilateral SFGdor, MFG, and SFGmed that are known to be primarily involved in strategic/executive functions (Duncan and Owen, 2000). 2) Module II is mainly composed of 24 cortical regions associated with auditory/language and mnemonic functions such as the STG, SMG, IFGoperc and parahippocampal gyrus (PHG) (Mesulam, 1990). 3) Module III includes 23 regions that are mostly linked with visual processing such as the bilateral SOG, MOG, IOG and lingual gyrus (LING). Interestingly, it can be further divided into two groups (frontal/occipital and temporal/occipital) of regions which are corresponding to the dorsal and ventral visual pathways (Grill-Spector, 2003), respectively (data not shown). 4) Module IV consists of 23 cortical regions that are mostly related to the sensorimotor/spatial functions such as bilateral PreCG, supplemental motor area (SMA), PoCG and SPG (Mesulam, 2000). Of note, the modular organization of both the young adults and normal aging brain networks uncovered here are largely in accordance with that of the young normal brain network obtained from our previous study (Chen et al., 2008).

Brain modularity: young adults vs. normal aging

We first examined the global modularity for both the young and normal aging brain structural networks (see Materials and methods). Five and four modules were detected in the young adults (Fig. 2A) and normal aging (Fig. 2B) groups, respectively. As expected, both networks exhibited strong modularity compared with those of the corresponding 1000 random networks ($P_{young}<0.001$, $P_{old}<0.001$). There was no significant difference detected in the global network modularity between the two cohorts, indicating conserved modular architecture in both the young and aging brain networks.

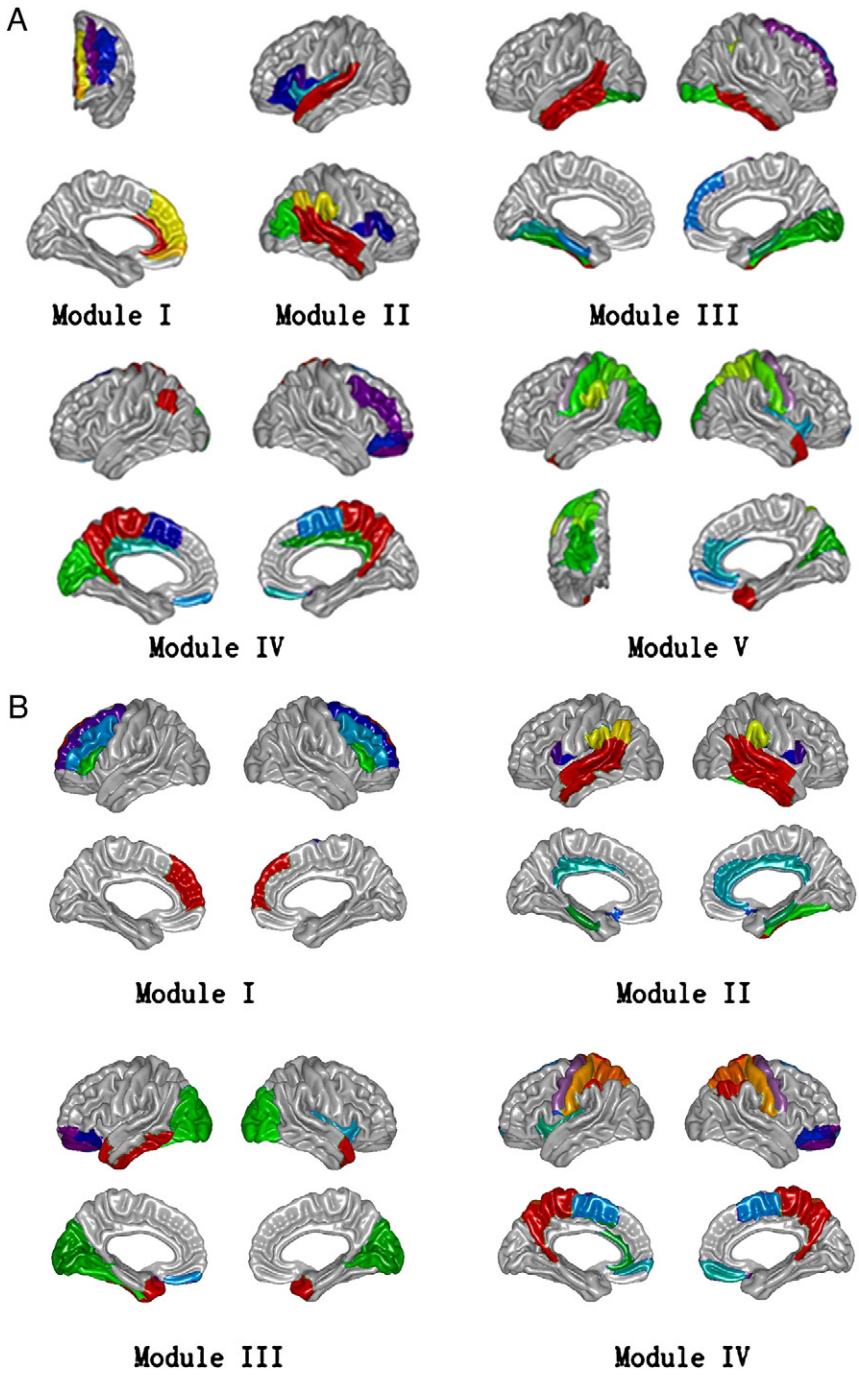

Fig. 2. Modular organization of the cortical structural network for both the young adults and normal aging populations. (A) The modular organization of young adults brain network. Module I: executive strategic. Module II: auditory/language. Module III: visual integration (ventral visual pathway). Module IV: default mode network. Module V: sensorimotor/visual/spatial. (B) The modular organization of normal aging brain network. Module I: executive strategic. Module II: auditory/language. Module III: visual (dorsal and ventral visual pathways). Module IV: sensorimotor/spatial.

Secondly, we presupposed that the modular organization for the young adults brain network (five modules, Fig. 2A) represents a more optimized design for the brain network. An important question raised from the altered modular structures in the normal aging brain network concerns what happened to this "ideal" modular organization in aging. Therefore, the network comparisons between the young and elder groups in our study are focused on the same modular organization (5 modules, Fig. 2A) derived from the young adults group. We applied this modular organization to the aging brain network and recalculated the modularity of the network. Though this modular organization corresponds to the maximum modularity in the young adult brain network, it yields a significant reduced modularity in the aging group (-53%, $p<0.001$) as shown in Fig. 3.

Alterations in the modular organization of aging structural brain network

We then examined alterations in the intra-module connectivity (MC) for all the five functional oriented modules obtained in the young adults brain network in aging (see Materials and methods). As shown in Fig. 4, when compared with the same modular structures of the young adult brain network, aging networks exhibited a significantly reduced

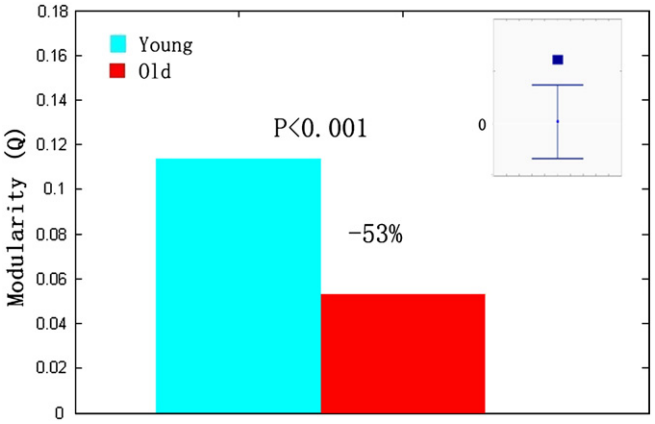

Fig. 3. Between-group difference in the network modularity. The network modularity of the aging group (red) is significantly reduced when compared with the young adults brain network (blue). The inset represents the mean values and 95% confidence intervals of the between-group differences obtained from 1000 permutation tests for the network modularity of both groups.

connectivity in both the strategic/executive module (module I, $p = 0.005$) and default mode network module (module IV, $p = 0.035$). A decreasing trend was also observed for the auditory/language module (module II, $p = 0.052$).

Next, we examined the age-related alterations in the inter-module connectivity (IMC). As shown in Fig. 5, we found a significantly reduced inter-module connectivity between the default mode network and executive/strategic modules (IV-I, $p = 0.047$) and increased connectivity between the default mode network and sensorimotor modules (IV-V, $p = 0.022$), respectively.

Age-related alterations in regional roles

We also explored the age-related alterations in the regional roles in terms of their intra- and inter-module connectivity (see Materials and methods). The within-module degree z_i, quantifies the connectedness of node i to other nodes in the module and the participation coefficient PC_i measures the weight distribution of node i among all the modules in the network. Fig. 6 demonstrated the alterations in the regional roles of the normal aging brain network compared with those of the young brains in

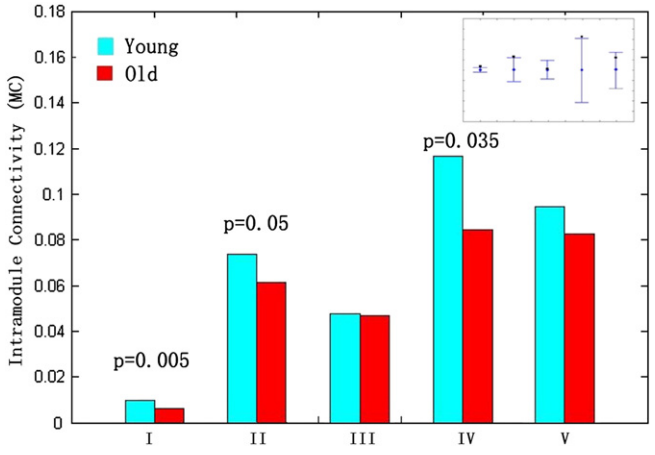

Fig. 4. Between-group difference in the intra-modular connectivity (MC). The graph demonstrated the difference in the connectivity of modular structures between the young adults (blue) and normal aging groups (red). Aging group showed a significantly reduced connectivity in the Module I, IV and a trend in II. I: executive/strategic, IV: default mode network , II: auditory/language. The inset represents the mean values and 95% confidence intervals of the between-group differences obtained from 1000 permutation tests for the 5 modules of the young adults brain network.

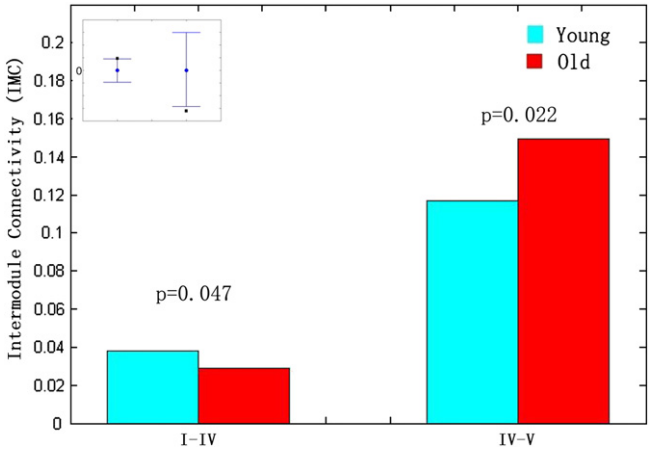

Fig. 5. Between-group difference in the inter-module connectivity. The graph demonstrated the difference in the inter-modular connectivity between the young adults (blue) and normal aging (red) groups. Aging group showed a significantly reduced connectivity between the modules I and IV (executive/strategic-default mode network) and increased connectivity between modules IV and V (default mode network—sensorimotor/visual/spatial). The inset represents the mean values and 95% confidence intervals of the between-group differences obtained from 1000 permutation tests for the inter-module connectivity of the young adults brain network.

PC (16 regions) and *Z* (12 regions) (red bar: Aging>Young, blue bar: Young>Aging).

We found that, compared with the young brain network, most altered roles in the aging brain network have an increased inter-module connectivity (14/16). The default mode network and sensorimotor/spatial modules are the two most affected modules as each has 5 regions with increased inter-modular connectivity. Twelve regions are found to have significantly altered and evenly distributed intra-modular connectivity across all the modular structures in the normal aging brain network (e.g., SFGmed/SFGdor in the executive module and PoCG in the sensorimotor/spatial module) which might be an indication of coordinated cognitive declines in normal aging.

Altered inter-regional correlations

Statistical analysis also revealed significant between-group differences in regional correlation strength ($p = 0.05$, FDR corrected) in 33 pairs of cortical regions (Table 2). While the number of increased and decreased correlations in normal aging brain network are similar (decrease/increase: 17/16), almost all decreases are among anterior–posterior regions (e.g. MFG/MOG, SFG/SOG) and within the default mode network module (e.g. PCG/PCUN, PCG/MCG) as shown in Table 2a and 2b, respectively. On the other hand, most increased inter-regional correlations are found to be involved with bilateral regions (e.g. SFGmed, PrCG) and intra/inter-lobule regions of occipital and parietal lobes (e.g. SOG/PCUN, SPG/PCUN, PoCG/PCL) as shown in the Table 2c and d, respectively.

Discussion

In the present study, we explored the effects of aging on the modular organization of large-scale structural brain networks using cortical thickness measurements. We applied a fully-weighted cortical network analysis to avoid the thresholding issue that can lead to inconsistent network properties over a wide range of sparsity in previous structural and functional brain networks studies in human (Achard and Bullmore, 2007; He et al., 2007, 2008; Gong et al., 2009). Our main results were that (1) compared with the modular structures derived from the young adult brain network, the normal aging network displayed a significantly reduced modularity; (2) with the exception of the default mode network module, most modular

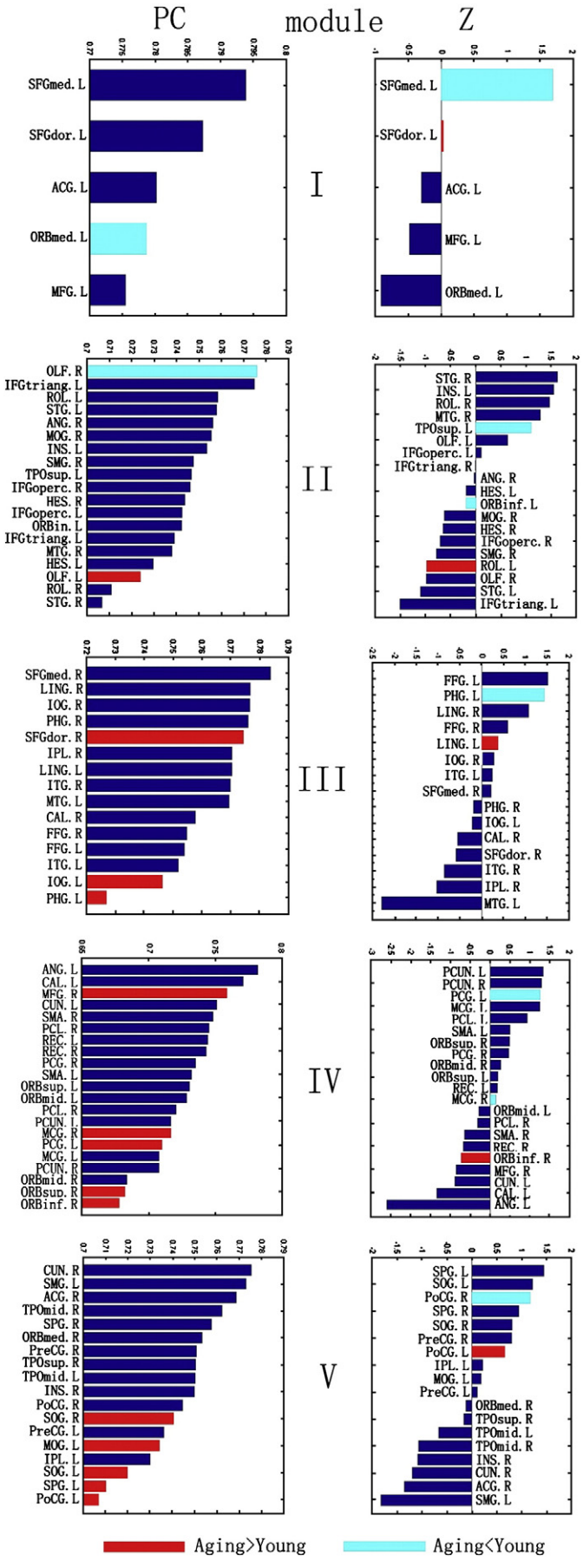

Table 2
Altered regional correlations in normal aging brain network. Bold: significant correlations ($p<0.05$, FDR corrected). a) decreased correlations among anterior-posterior cortical regions. b) decreased correlations within the default mode network module. c) increased correlations among bilateral frontal regions. d) increased correlations among intra/inter-lobular regions of occipital and parietal lobes.

Regions	Regions	Regional correlation *R*			
		Young	Old	*Z* score	
Decreased R in aging					
Rolandic_Oper_R	Parietal_Sup_L	0.08	**−0.45**	3.86	
Rolandic_Oper_L	Parietal_Sup_L	0.18	**−0.35**	3.78	
Frontal_Sup_Medial_R	Precuneus_L	0.15	**−0.37**	3.75	
Precentral_R	Occipital_Mid_L	**0.43**	−0.08	3.74	
Frontal_Mid_Orb_L	Parietal_Inf_L	0.02	**−0.47**	3.68	
Frontal_Sup_L	Occipital_Sup_L	0.12	**−0.39**	3.68	(a)
Rolandic_Oper_R	ParaHippocampal_L	0.19	**−0.45**	4.70	
Frontal_Inf_Orb_R	Postcentral_L	0.04	**−0.50**	4.11	
Rolandic_Oper_R	Parietal_Sup_R	0.09	**−0.38**	3.43	
Frontal_Mid_Orb_L	Occipital_Mid_L	0.09	**−0.37**	3.29	
Frontal_Mid_R	Occipital_Mid_L	0.11	**−0.35**	3.28	
Frontal_Mid_R	Occipital_Sup_L	0.04	**−0.40**	3.27	
Cingulum_Post_L	Precuneus_L	**0.68**	0.08	5.18	
Cingulum_Post_R	Precuneus_L	**0.51**	−0.10	4.58	
Cingulum_Mid_R	Cingulum_Post_L	**0.56**	0.10	3.67	(b)
Cingulum_Post_L	Cingulum_Post_R	**0.75**	0.45	3.44	
Cingulum_Post_L	Precuneus_R	**0.45**	0.00	3.32	
Increased R in aging					
Frontal_Sup_Medial_L	Frontal_Sup_Medial_R	**0.49**	**0.80**	−4.01	
Precentral_L	Precentral_R	**0.47**	**0.75**	−3.25	
Precentral_R	Supp_Motor_Area_L	0.01	**0.50**	−3.73	(c)
Frontal_Inf_Orb_L	Temporal_Mid_R	**−0.47**	−0.05	−3.20	
Precentral_R	Paracentral_Lobule_L	0.07	**0.59**	−4.24	
Occipital_Sup_L	Precuneus_L	−0.25	**0.44**	−5.10	
Parietal_Sup_L	Precuneus_L	0.01	**0.62**	−4.94	
Parietal_Inf_L	Precuneus_L	−0.23	**0.42**	−4.74	
Occipital_Mid_L	Precuneus_L	−0.20	**0.38**	−4.17	
Temporal_Pole_Sup_R	Temporal_Pole_Mid_R	**0.43**	**0.77**	−3.84	(d)
Lingual_L	Fusiform_L	0.28	**0.67**	−3.63	
Parietal_Sup_R	Precuneus_L	0.04	**0.49**	−3.44	
Parietal_Inf_L	Parietal_Inf_R	0.11	**0.54**	−3.39	
Occipital_Sup_R	Precuneus_L	−0.09	**0.37**	−3.27	
Rectus_L	Cingulum_Post_L	**−0.37**	0.08	−3.26	
Postcentral_R	Paracentral_Lobule_L	0.12	**0.52**	−3.16	

structures are well preserved in normal aging; (3) observed altered intra/inter-module connectivity among the modules associated with executive/strategic functions and the default mode network; (4) the regional roles in terms of their intra- and inter-module connectivity are also affected in aging population; and (5) regional connectivity analysis revealed disruptions between anterior and posterior brain regions and within the default mode network module.

Reduced modularity in the normal aging brain network

Recent studies have consistently demonstrated that the normal human brain functional and structural networks exhibit a modular topological organization (Salvador et al., 2005; Chen et al., 2008; Ferrarini et al., 2009; Hagmann et al., 2008; He et al., 2009).

It has been suggested that the modular organization of the cortical network provides a balance between the two most fundamental aspects of brain organization: functional segregation and integration

Fig. 6. Altered regional roles in the normal aging brain network compared to those of the young adults brain network. The participation coefficient (*PC*) of each cortical region for the young adults brain network which measures the weight distribution of a region among all the modules in the network is shown in the left column. The within-module degree (*z*) of each cortical region for the young adults brain network which quantifies the connectedness of a region to other region in the module is listed in the right column. The between-group comparisons identified 16 and 12 regions with significant altered PC and *Z* values in the normal aging brain network, respectively (red: Aging>Young adults, blue: Young adults>Aging).

(Sporns et al., 2004). It represents a general network organizational principle and may contribute to the efficient recurrent processing within modules (Sporns et al., 2000; Kotter and Stephan, 2003), and information exchange between modules (Latora and Marchiori, 2001). Our findings of high global modularity in both young adult and normal aging structural networks are in accordance with previous studies as both networks attempt to maintain an optimal balance between the local specialization and global integration of the information process.

However, while comparing with the same modular structures of the young adult brain, the normal aging network demonstrated significantly reduced modularity (Fig. 2). Previous studies have demonstrated various aging effects on the brain ranging from morphological abnormalities such as decreased grey matter density (Sowell et al., 2003) to cortical thickness (Salat et al., 2004; Fjell et al., 2009), and alterations in functional/structural brain systems (Grady et al., 2003; Salat et al., 2005; Andrews-Hanna et al., 2007). Furthermore, the normal aging structural and functional brain networks have been shown to display altered characteristics such as decreased local and global efficiency that are essential in sustaining both the segregated and integrated information processing in the normal brain system (Achard and Bullmore, 2007; Gong et al., 2009). It is likely that the reduced modularity in the normal aging brain network arises from the re-organization of the brain network in order to offset the age-related focal abnormalities such as widespread cortical thinning (Supplemental Fig. 1) and maintain stable cognitive functions.

Altered modular organization of the cortical structural network in aging

We identified 5 and 4 modules (Figs. 2A & B) that correspond to several different brain functional domains in the young adult and normal aging groups, respectively. Those results are compatible with the functional modules detected in the mammalian anatomical network (Scannell et al., 1999; Hilgetag et al., 2000a; Zhou et al., 2006) and human brain functional networks using fMRI (Salvador et al., 2005; Meunier et al., 2009). More importantly, it is also largely consistent with our previous study on the modular organization of human brain structural network constructed from regional cortical thickness measurements in normal adults (Chen et al., 2008). The well preserved function-oriented modular organization in aging might be associated with a relatively slower decline in the key cognitive abilities such as memory, vocabulary and previously acquired skills in normal aging when compared with those of the neurodegenerative diseases such as AD (Drachman, 2006).

Notwithstanding this preservation, there were some notable differences between the two groups. First, the reduced number of modules detected in aging might reflect a loss of functional segregation as more regions are grouped together to achieve certain functions (Sporns et al., 2004). For example, in the executive/strategic modules of both groups, only left-hemispheric frontal regions were grouped together in the young adult network as opposed to all bilateral frontal regions in the aging network. A recent study has suggested a model of aging effects on brain activity during cognitive performance, dubbed HAROLD (hemispheric asymmetry reduction in older adults). It states that, under similar circumstances, prefrontal activity during cognitive performances tends to be less lateralized in older adults than in younger adults (Cabeza, 2002). Since then, age-related over-activation in the right-hemispheric frontal regions have been reported in several studies (Cabeza et al., 2002; Grady et al., 2010; Park and Reuter-Lorenz, 2009). Our finding of reduced modularity in executive module for older subjects is consistent with the HAROLD model.

We also found age-related decreases in the connectivity of the executive/strategic and default mode network modules (Fig. 2). This is intriguing since impairments in brain functions such as executive and memory are the main characteristics of aging and have been well documented in many studies (Buckner, 2004; Park and Reuter-Lorenz, 2009; Madden et al., 2010). The reduced connectivity of the default mode network module (DMN) is particularly interesting, as the DMN is a set of brain regions reported to be active in rest and deactivated in task states (Shulman et al., 1997; Fox and Raichle, 2007). The DMN is part of a resting-state brain network that has been suggested to reflect an intrinsic property of brain functional organization that serves to stabilize brain ensembles (Raichle and Snyder, 2007; Damoiseaux et al., 2008). Recent studies have demonstrated decreased DMN activity at rest in the normal aging population when compared with the young subjects (Damoiseaux et al., 2008; Grady et al., 2010). Thus, we could speculate that the reduced connectivity of the modules in the aging network might be related to the decline of cognitive functions (e.g. executive control) and reduced DMN activity in aging.

We observed significantly decreased connectivity between the executive and DMN modules. Previous studies have suggested that cognitive declines in normal aging might be associated with a disconnection of neural networks necessary for efficient cognitive performance (O'Sullivan et al., 2001). Specifically, brain diffusion tensor imaging (DTI) studies have supported an anterior–posterior gradient of age-related decline in white matter integrity (FA) where the frontal regions have demonstrated the most significant decreases (Salat et al., 2005; Madden et al., 2009). In 2007, Andrews-Hanna et al. also demonstrated that reduced functional correlations between the anterior and posterior components of the default network might be associated with disruptions in white matter integrity and poor cognitive performance. More importantly, Meunier et al. (2009) reported a loss of functional connectivity between the frontal and posterior temporal parietal clusters in normal aging. Thus, the disrupted connectivity between the frontal and posterior parts of the brain observed in our study indicate a structural disconnection between the two of the most essential brain functional networks, the executive and default mode networks, in normal aging. On the other hand, the connectional strength between the sensorimotor/spatial and DMN modules was shown to be significantly increased. This might be attributed to increased regional connectivity (Table 2d) between the posterior components of the default mode network and sensorimotor/visual/spatial modules (e.g. PCUN/SOG, PCUN/SPL). Posterior parietal regions such as PCUN are key regions of the default mode network in young adults (Raichle et al., 2001; Greicius et al., 2003) and have been found to show age-related increased activity with aging during task (e.g. PCUN) (Lustig et al., 2003; Grady et al., 2006; Wang et al., 2010). However, the underlying neurobiological mechanism of such disconnections, such as demyelination and axonal loss, are still unclear.

Altered regional roles in the normal aging

We found age-related alterations in the regional roles in terms of their intra- and inter-module connectivity pattern. Compared with the young adult network, most regional inter-module connectivity (*PC*, see Materials and methods) changes are positive, implying an increased inter-module recruitment of regions in the aging brain network. Regions showing increased inter-module connectivity are mostly located in right frontal lobe (e.g. SFGdor, MFG) and the default mode network (e.g. PCG, ORBsup) and sensorimotor/visual/spatial modules (e.g. SPG, SOG). Interestingly, age-related overactivation in the right-hemispheric frontal regions, posterior DMN and lateral parietal regions across a variety of cognitive tasks has been well documented (Cabeza et al., 2002; Lustig et al., 2003; Damoiseaux et al., 2008; Grady et al., 2010; Park and Reuter-Lorenz, 2009). Thus, we speculate that age-related increases in regional inter-module connectivity might reflect the functional recruitment of those brain areas in normal aging (e.g. executive control) (Buckner, 2004) to meet task demands. On the other hand, we also observed altered regional intra-module connectivity (*Z*) with age. Surprisingly, the normal aging brain

network displayed well-balanced and distributed intra-module connectivity changes across all the modular structures as shown in Fig. 5. This might represent a compensatory process such as the scaffolding mechanism (Park and Reuter-Lorenz, 2009) that underlies the relatively well preserved cognitive functions in normal aging when compared with those of brain diseases such as AD (Drachman, 2006).

Altered inter-regional correlations in aging

One of the fundamental mechanisms of modular re-organization in normal aging is the alteration in inter-regional correlations. We observed significantly altered correlation among various cortical regions (Table 2). Almost all decreased inter-regional correlations were between the anterior (frontal) and posterior (parietal/occipital) brain regions (Table 2a) and within the DMN module (Table 2b). These results are consistent with many functional brain network studies that show age-related alterations in frontal–occipital (Wang et al., 2010) and frontal–parietal (Buckner, 2004; Meunier et al., 2009) connectivity. Declines in the white matter integrity of anterior–posterior fibre tracts (e.g. superior longitudinal fasciculus) also have been found to contribute to a disconnection among distributed brain systems that lead to various functional deficits in aging (Davis et al., 2009; Madden et al., 2009). Similarly, the DMN of the resting state network has been shown to have decreased activity in normal aging (Damoiseaux et al., 2008; Grady et al., 2010). Thus, the reduced interregional connectivity observed here might provide further structural evidences to support the anterior–posterior disconnection aging model (Grady et al., 2001) and reduced DMN connectivity in aging (Grady et al., 2010).

In contrast, most increased inter-regional correlations were found to involve bilateral frontal (Table 2c) and posterior (Table 2d) brain regions. Increased inter-regional correlations might be an indication of increased functional connectivity among those regions. In normal aging, overactivation is often found in the frontal regions that mirror active sites in young adults but in the opposite hemisphere known as the HAROLD model (Cabeza, 2002; Reuter-Lorenz and Cappell, 2008). Thus, the increased inter-hemispheric structural connectivity observed here might reflect an increased functional connectivity between bilateral frontal regions in the aging brain as it attempts to maintain a stable functional state according to the HAROLD principle. Posterior brain regions such as PCUN are the vital regions in the DMN network (Raichle et al., 2001; Greicius et al., 2003) and have been found to show increased activity in aging during tasks (Lustig et al., 2003; Grady et al., 2010). Therefore increased structural correlation among posterior brain regions may also reflect this increased functional connectivity in aging.

Methodological issues

One caveat to consider in this study is that the underlying biological nature of the morphological correlations among brain regions (e.g. cortical thickness) is still unknown. It has been suggested that the correlated covariation of the morphological features might result from mutually trophic influences (Ferrer et al., 1995), the contribution of heredity (Suddath et al., 1990; Thompson et al., 2001) or common experience-related plasticity (Mechelli et al., 2005). The other limitation of our approach is that the inter-regional correlation matrix for each group was population-based. Thus, we could not explore the modular organization for individual subjects. However, resting fMRI and diffusion MRI can deal with individual data as one network is generated for each subject. Third, cortical regions in our present study are defined by the AAL atlas which provides a more detailed and biological meaningful set of cortical regions (AAL) than our previous one (He et al., 2008). However, the use of different parcellation schemes might cause subtle change of network organization (Wang et al., 2009), though the essential modular architecture for any cortical parcellation based on commonly accepted gyral/lobar boundaries should remain intact. A more specific limitation is the uneven gender distribution in the young adults and elder groups. Functional brain network studies have detected large sex-related variations in the resting state fMRI measures of brain functional connectivity (Biswal et al., 2010). However, in a recent gender-related cortical thickness network study (Lv et al., 2010), both male and female population have demonstrated a similar structural (cortical thickness) connectivity pattern. In our study, we tried to remove the gender effect by using the regression model. Nevertheless, future studies with gender specific groups would be more appropriate. Finally, in our study, we only compared the modular structures of young adults between the young and elder groups, thus it might yield a more biased result as the brain functional networks tend to change in aging (Greenwood, 2007). In the future study, comparison between modular organizations based on a population-based brain map would be more appropriate.

In conclusion, we used regional cortical thickness measurements to demonstrate, for the first time, age-related alterations in the modular organization of the human brain structural networks. We demonstrated a reduced intra-module connectivity in the executive functional and DMN modules, as well as decreased inter-module connectivity between anterior and posterior modules. We also examined the alteration in regional intra/inter-module connectivity that might reflect the underlying compensatory mechanism in aging brain. Our findings are compatible with the notion that aging is associated with structural and functional disconnection among different brain systems. The present study has implications for understanding how the modular organizational alterations in the large-scale brain networks underlie functional deficits in aging.

Supplementary data to this article can be found online at doi:10.1016/j.neuroimage.2011.01.010.

References

Achard, S., Bullmore, E., 2007. Efficiency and cost of economical brain functional networks. PLoS Comput. Biol. 3, e17.

Andrews-Hanna, J.R., Snyder, A.Z., Vincent, J.L., Lustig, C., Head, D., Raichle, M.E., Buckner, R.L., 2007. (Disruption of large-scale brain systems in advanced aging. Neuron 56, 924–935.

Biswal, B.B., Mennes, M., Zuo, X.N., Gohel, S., Kelly, C., Smith, S.M., Beckmann, C.F., Adelstein, J.S., Buckner, R.L., Colcombe, S., Dogonowski, A.M., Ernst, M., Fair, D., Hampson, M., Hoptman, M.J., Hyde, J.S., Kiviniemi, V.J., Kotter, R., Li, S.J., Lin, C.P., Lowe, M.J., Mackay, C., Madden, D.J., Madsen, K.H., Margulies, D.S., Mayberg, H.S., McMahon, K., Monk, C.S., Mostofsky, S.H., Nagel, B.J., Pekar, J.J., Peltier, S.J., Petersen, S.E., Riedl, V., Rombouts, S.A., Rypma, B., Schlaggar, B.L., Schmidt, S., Seidler, R.D., Siegle, G.J., Sorg, C., Teng, G.J., Veijola, J., Villringer, A., Walter, M., Wang, L., Weng, X.C., Whitfield-Gabrieli, S., Williamson, P., Windischberger, C., Zang, Y.F., Zhang, H.Y., Castellanos, F.X., Milham, M.P., 2010. Toward discovery science of human brain function. Proc. Natl Acad. Sci. USA 107, 4734–4739.

Buckner, R.L., 2004. Memory and executive function in aging and AD: multiple factors that cause decline and reserve factors that compensate. Neuron 44, 195–208.

Bullmore, E.T., Suckling, J., Overmeyer, S., Rabe-Hesketh, S., Taylor, E., Brammer, M.J., 1999. Global, voxel, and cluster tests, by theory and permutation, for a difference between two groups of structural MR images of the brain. IEEE Trans. Med. Imaging 18, 32–42.

Cabeza, R., 2002. Hemispheric asymmetry reduction in older adults: the HAROLD model. Psychol. Aging 17, 85–100.

Cabeza, R., Anderson, N.D., Locantore, J.K., McIntosh, A.R., 2002. Aging gracefully: compensatory brain activity in high-performing older adults. Neuroimage 17, 1394–1402.

Chen, Z.J., He, Y., Rosa-Neto, P., Germann, J., Evans, A.C., 2008. Revealing modular architecture of human brain structural networks by using cortical thickness from MRI. Cereb. Cortex 18, 2374–2381.

Clauset, A., Newman, M.E., Moore, C., 2004. Finding community structure in very large networks. Phys. Rev. 70, 066111.

Cohen, J., Cohen, P., 1983. Applied multiple regression/correlation analysis for the behavioral sciences. Erlbaum, Hillsdale NJ.

Collins, D.L., Holmes, C.J., Peter, T.M., Evans, A.C., 1995. Automatic 3D model-based neuroanatomical segmentation. Hum. Brain Mapp. 33, 190–208.

Collins, D.L., Neelin, P., Peters, T.M., Evans, A.C., 1994. Automatic 3D intersubject registration of MR volumetric data in standardized Talairach space. J. Comput. Assist. Tomogr. 18, 192–205.

Damoiseaux, J.S., Beckmann, C.F., Arigita, E.J., Barkhof, F., Scheltens, P., Stam, C.J., Smith, S.M., Rombouts, S.A., 2008. Reduced resting-state brain activity in the "default network" in normal aging. Cereb. Cortex 18, 1856–1864.

Danon, L., Diaz-Guilera, A., Arenas, A., 2006. The effect of size heterogeneity on community identification in complex networks. J. Stat. Mech.: Theory Exp. P11010.
Davis, S.W., Dennis, N.A., Buchler, N.G., White, L.E., Madden, D.J., Cabeza, R., 2009. Assessing the effects of age on long white matter tracts using diffusion tensor tractography. Neuroimage 46, 530–541.
Drachman, D.A., 2006. Aging of the brain, entropy, and Alzheimer disease. Neurology 67, 1340–1352.
Duncan, J., Owen, A.M., 2000. Common regions of the human frontal lobe recruited by diverse cognitive demands. Trends Neurosci. 23, 475–483.
Ferrarini, L., Veer, I.M., Baerends, E., van Tol, M.J., Renken, R.J., van der Wee, N.J., Veltman, D.J., Aleman, A., Zitman, F.G., Penninx, B.W., van Buchem, M.A., Reiber, J.H., Rombouts, S.A., Milles, J., 2009. Hierarchical functional modularity in the resting-state human brain. Hum. Brain Mapp. 30, 2220–2231.
Ferrer, I., Blanco, R., Carulla, M., Condom, M., Alcantara, S., Olive, M., Planas, A., 1995. Transforming growth factor-alpha immunoreactivity in the developing adult brain. Neuroscience 66, 189–199.
Fjell, A.M., Westlye, L.T., Amlien, I., Espeseth, T., Reinvang, I., Raz, N., Agartz, I., Salat, D.H., Greve, D.N., Fischl, B., Dale, A.M., Walhovd, K.B., 2009. High consistency of regional cortical thinning in aging across multiple samples. Cereb. Cortex 19, 2001–2012.
Fortunato, S., Barthelemy, M., 2007. Resolution limit in community detection. Proc. Natl Acad. Sci. USA 104, 36–41.
Fox, M.D., Raichle, M.E., 2007. Spontaneous fluctuations in brain activity observed with functional magnetic resonance imaging. Nat. rev. 8, 700–711.
Genovese, C.R., Lazar, N.A., Nichols, T., 2002. Thresholding of statistical maps in functional neuroimaging using the false discovery rate. Neuroimage 15, 870–878.
Gong, G., He, Y., Concha, L., Lebel, C., Gross, D.W., Evans, A.C., Beaulieu, C., 2009. Mapping anatomical connectivity patterns of human cerebral cortex using in vivo diffusion tensor imaging tractography. Cereb. Cortex 19, 524–536.
Grady, C.L., Furey, M.L., Pietrini, P., Horwitz, B., Rapoport, S.I., 2001. Altered brain functional connectivity and impaired short-term memory in Alzheimer's disease. Brain 124, 739–756.
Grady, C.L., McIntosh, A.R., Beig, S., Keightley, M.L., Burian, H., Black, S.E., 2003. Evidence from functional neuroimaging of a compensatory prefrontal network in Alzheimer's disease. J. Neurosci. 23, 986–993.
Grady, C.L., Protzner, A.B., Kovacevic, N., Strother, S.C., Afshin-Pour, B., Wojtowicz, M., Anderson, J.A., Churchill, N., McIntosh, A.R., 2010. A multivariate analysis of age-related differences in default mode and task-positive networks across multiple cognitive domains. Cereb. Cortex 20, 1432–1447.
Grady, C.L., Springer, M.V., Hongwanishkul, D., McIntosh, A.R., Winocur, G., 2006. Age-related changes in brain activity across the adult lifespan. J. Cogn. Neurosci. 18, 227–241.
Greenwood, P.M., 2007. Functional plasticity in cognitive aging: review and hypothesis. Neuropsychology 21, 657–673.
Greicius, M.D., Krasnow, B., Reiss, A.L., Menon, V., 2003. Functional connectivity in the resting brain: a network analysis of the default mode hypothesis. Proc. Natl Acad. Sci. USA 100, 253–258.
Grill-Spector, K., 2003. The neural basis of object perception. Curr. Opin. Neurobiol. 13, 159–166.
Guimera, R., Amaral, L.A., 2005. Cartography of complex networks: modules and universal roles. J. stat. mech. 2005 (P02001), 1–13.
Guimera, R., Mossa, S., Turtschi, A., Amaral, L.A., 2005. The worldwide air transportation network: anomalous centrality, community structure, and cities' global roles. Proc. Natl Acad. Sci. USA 102, 7794–7799.
Guimera, R., Nunes Amaral, L.A., 2005. Functional cartography of complex metabolic networks. Nature 433, 895–900.
Hagmann, P., Cammoun, L., Gigandet, X., Meuli, R., Honey, C.J., Wedeen, V.J., Sporns, O., 2008. Mapping the structural core of human cerebral cortex. PLoS Biol. 6, e159.
He, Y., Chen, Z., Evans, A., 2008. Structural insights into aberrant topological patterns of large-scale cortical networks in Alzheimer's disease. J. Neurosci. 28, 4756–4766.
He, Y., Chen, Z.J., Evans, A.C., 2007. Small-world anatomical networks in the human brain revealed by cortical thickness from MRI. Cereb. Cortex 17, 2407–2419.
He, Y., Wang, J., Wang, L., Chen, Z.J., Yan, C., Yang, H., Tang, H., Zhu, C., Gong, Q., Zang, Y., Evans, A., 2009. Uncovering intrinsic modular organization of spontaneous brain activity in humans. PloS ONE 4, e5226.
Hilgetag, C.C., Burns, G.A., O'Neill, M.A., Scannell, J.W., Young, M.P., 2000a. Anatomical connectivity defines the organization of clusters of cortical areas in the macaque monkey and the cat. Philos. Trans. R. Soc. Lond. 355, 91–110.
Hilgetag, C.C., O'Neill, M.A., Young, M.P., 2000b. Hierarchical organization of macaque and cat cortical sensory systems explored with a novel network processor. Philos. Trans. R. Soc. Lond. 355, 71–89.
Ison, M.J., Quiroga, R.Q., 2008. Selectivity and invariance for visual object perception. Front. Biosci. 13, 4889–4903.
Kashtan, N., Alon, U., 2005. Spontaneous evolution of modularity and network motifs. Proc. Natl Acad. Sci. USA 102, 13773–13778.
Kim, J.S., Singh, V., Lee, J.K., Lerch, J., Ad-Dab'bagh, Y., MacDonald, D., Lee, J.M., Kim, S.I., Evans, A.C., 2005. Automated 3-D extraction and evaluation of the inner and outer cortical surfaces using a Laplacian map and partial volume effect classification. Neuroimage 27, 210–221.
Kotter, R., Stephan, K.E., 2003. Network participation indices: characterizing component roles for information processing in neural networks. Neural Netw. 16, 1261–1275.
Latora, V., Marchiori, M., 2001. Efficient behavior of small-world networks. Phys. Rev. Lett. 87, 198701.
Lerch, J.P., Evans, A.C., 2005. Cortical thickness analysis examined through power analysis and a population simulation. Neuroimage 24, 163–173.
Lustig, C., Snyder, A.Z., Bhakta, M., O'Brien, K.C., McAvoy, M., Raichle, M.E., Morris, J.C., Buckner, R.L., 2003. Functional deactivations: change with age and dementia of the Alzheimer type. Proc. Natl Acad. Sci. USA 100, 14504–14509.
Lv, B., Li, J., He, H., Li, M., Zhao, M., Ai, L., Yan, F., Xian, J., Wang, Z., 2010. Gender consistency and difference in healthy adults revealed by cortical thickness. Neuroimage 53, 373–382.
MacDonald, D., Kabani, N., Avis, D., Evans, A.C., 2000. Automated 3-D extraction of inner and outer surfaces of cerebral cortex from MRI. Neuroimage 12, 340–356.
Madden, D.J., Bennett, I.J., Song, A.W., 2009. Cerebral white matter integrity and cognitive aging: contributions from diffusion tensor imaging. Neuropsychol. Rev. 19, 415–435.
Madden, D.J., Costello, M.C., Dennis, N.A., Davis, S.W., Shepler, A.M., Spaniol, J., Bucur, B., Cabeza, R., 2010. Adult age differences in functional connectivity during executive control. Neuroimage 52, 643–657.
Marcus, D.S., Wang, T.H., Parker, J., Csernansky, J.G., Morris, J.C., Buckner, R.L., 2007. Open Access Series of Imaging Studies (OASIS): cross-sectional MRI data in young, middle aged, nondemented, and demented older adults. J. Cogn. Neurosci. 19, 1498–1507.
Mechelli, A., Friston, K.J., Frackowiak, R.S., Price, C.J., 2005. Structural covariance in the human cortex. J. Neurosci. 25, 8303–8310.
Mesulam, M.M., 1990. Large-scale neurocognitive networks and distributed processing for attention, language, and memory. Ann. Neurol. 28, 597–613.
Mesulam, M.M., 2000. Principles of behavioral and cognitive. Oxford University Press, New York, pp. 1–91.
Meunier, D., Achard, S., Morcom, A., Bullmore, E., 2009. Age-related changes in modular organization of human brain functional networks. Neuroimage 44, 715–723.
Morris, J.C., 1993. The Clinical Dementia Rating (CDR): current version and scoring rules. Neurology 43, 2412–2414.
Morris, J.C., Storandt, M., Miller, J.P., McKeel, D.W., Price, J.L., Rubin, E.H., Berg, L., 2001. Mild cognitive impairment represents early-stage Alzheimer disease. Arch. Neurol. 58, 397–405.
Newman, M.E., 2004. Analysis of weighted networks. Phys. Rev. 70, 056131.
O'Sullivan, M., Jones, D.K., Summers, P.E., Morris, R.G., Williams, S.C., Markus, H.S., 2001. Evidence for cortical "disconnection" as a mechanism of age-related cognitive decline. Neurology 57, 632–638.
Park, D.C., Reuter-Lorenz, P., 2009. The adaptive brain: aging and neurocognitive scaffolding. Annu. Rev. Psychol. 60, 173–196.
Raichle, M.E., MacLeod, A.M., Snyder, A.Z., Powers, W.J., Gusnard, D.A., Shulman, G.L., 2001. A default mode of brain function. Proc. Natl Acad. Sci. USA 98, 676–682.
Raichle, M.E., Snyder, A.Z., 2007. A default mode of brain function: a brief history of an evolving idea. Neuroimage 37, 1083–1090 discussion 1097-1089.
Reuter-Lorenz, P.A., Cappell, K.A., 2008. Neurocognitive aging and the compensation hypothesis. Curr. Dir. Psychol. Sci. 17.
Robbins, S., Evans, A.C., Collins, D.L., Whitesides, S., 2004. Tuning and comparing spatial normalization methods. Med. Image Anal. 8, 311–323.
Salat, D.H., Buckner, R.L., Snyder, A.Z., Greve, D.N., Desikan, R.S., Busa, E., Morris, J.C., Dale, A.M., Fischl, B., 2004. Thinning of the cerebral cortex in aging. Cereb. Cortex 14, 721–730.
Salat, D.H., Tuch, D.S., Greve, D.N., van der Kouwe, A.J., Hevelone, N.D., Zaleta, A.K., Rosen, B.R., Fischl, B., Corkin, S., Rosas, H.D., Dale, A.M., 2005. Age-related alterations in white matter microstructure measured by diffusion tensor imaging. Neurobiol. Aging 26, 1215–1227.
Sales-Pardo, M., Guimera, R., Moreira, A.A., Amaral, L.A., 2007. Extracting the hierarchical organization of complex systems. Proc. Natl Acad. Sci. USA 104, 15224–15229.
Salvador, R., Suckling, J., Coleman, M.R., Pickard, J.D., Menon, D., Bullmore, E., 2005. Neurophysiological architecture of functional magnetic resonance images of human brain. Cereb. Cortex 15, 1332–1342.
Scannell, J.W., Burns, G.A., Hilgetag, C.C., O'Neil, M.A., Young, M.P., 1999. The connectional organization of the cortico-thalamic system of the cat. Cereb. Cortex 9, 277–299.
Seeley, W.W., Crawford, R.K., Zhou, J., Miller, B.L., Greicius, M.D., 2009. Neurodegenerative diseases target large-scale human brain networks. Neuron 62, 42–52.
Shulman, G.L., Corbetta, M., Buckner, R.L., Raichle, M.E., Fiez, J.A., Miezin, F.M., Petersen, S.E., 1997. Top-down modulation of early sensory cortex. Cereb. Cortex 7, 193–206.
Sled, J.G., Zijdenbos, A.P., Evans, A.C., 1998. A nonparametric method for automatic correction of intensity nonuniformity in MRI data. IEEE Trans. Med. Imaging 17, 87–97.
Sowell, E.R., Peterson, B.S., Thompson, P.M., Welcome, S.E., Henkenius, A.L., Toga, A.W., 2003. Mapping cortical change across the human life span. Nat. Neurosci. 6, 309–315.
Sporns, O., Chialvo, D.R., Kaiser, M., Hilgetag, C.C., 2004. Organization, development and function of complex brain networks. Trends Cogn. Sci. 8, 418–425.
Sporns, O., Tononi, G., Edelman, G.M., 2000. Theoretical neuroanatomy: relating anatomical and functional connectivity in graphs and cortical connection matrices. Cereb. Cortex 10, 127–141.
Suddath, R.L., Christison, G.W., Torrey, E.F., Casanova, M.F., Weinberger, D.R., 1990. Anatomical abnormalities in the brains of monozygotic twins discordant for schizophrenia. N. Engl. J. Med. 322, 789–794.
Thompson, P.M., Cannon, T.D., Narr, K.L., van Erp, T., Poutanen, V.P., Huttunen, M., Lonnqvist, J., Standertskjold-Nordenstam, C.G., Kaprio, J., Khaledy, M., Dail, R., Zoumalan, C.I., Toga, A.W., 2001. Genetic influences on brain structure. Nat. Neurosci. 4, 1253–1258.
Tzourio-Mazoyer, N., Landeau, B., Papathanassiou, D., Crivello, F., Etard, O., Delcroix, N., Mazoyer, B., Joliot, M., 2002. Automated anatomical labeling of activations in SPM using a macroscopic anatomical parcellation of the MNI MRI single-subject brain. Neuroimage 15, 273–289.

Valencia, M., Pastor, M.A., Fernandez-Seara, M.A., Artieda, J., Martinerie, J., Chavez, M., 2009. Complex modular structure of large-scale brain networks. Chaos 19 (023119) Woodbury, NY.

Variano, E.A., McCoy, J.H., Lipson, H., 2004. Networks, dynamics, and modularity. Phys. Rev. Lett. 92, 188701.

Wang, J., Wang, L., Zang, Y., Yang, H., Tang, H., Gong, Q., Chen, Z., Zhu, C., He, Y., 2009. Parcellation-dependent small-world brain functional networks: a resting-state fMRI study. Hum. Brain Mapp. 30, 1511–1523.

Wang, L., Li, Y., Metzak, P., He, Y., Woodward, T.S., 2010. Age-related changes in topological patterns of large-scale brain functional networks during memory encoding and recognition. Neuroimage 50, 862–872.

Watts, D.J., Strogatz, S.H., 1998. Collective dynamics of "small-world" networks. Nature 393, 440–442.

Zhou, C., Zemanova, L., Zamora, G., Hilgetag, C.C., Kurths, J., 2006. Hierarchical organization unveiled by functional connectivity in complex brain networks. Phys. Rev. Lett. 97, 238103.

Zhu, W., Wen, W., He, Y., Xia, A., Anstey, K.J., Sachdev, P., 2010. Changing topological patterns in normal aging using large-scale structural networks. Neurobiol. Aging. doi:10.1016/j.neurobiolaging.2010.06.022.

Zijdenbos, A.P., Forghani, R., Evans, A.C., 2002. Automatic "pipeline" analysis of 3-D MRI data for clinical trials: application to multiple sclerosis. IEEE Trans. Med. Imaging 21, 1280–1291.